HHS Public Access

Author manuscript

Biomaterials. Author manuscript; available in PMC 2024 October 07.

Published in final edited form as:

Biomaterials. 2022 July ; 286: 121601. doi:10.1016/j.biomaterials.2022.121601.

Host type 2 immune response to xenogeneic serum components impairs biomaterial-directed osteo-regenerative therapies

Karen E. Martin[1,2], **Pranav P. Kalelkar**[1,2], **María M. Coronel**[1,2], **Hannah S. Theriault**[3], **Rebecca S. Schneider**[2,4], **Andrés J. García**[1,2,*]

[1]Woodruff School of Mechanical Engineering, Georgia Institute of Technology, Atlanta, GA, USA

[2]Petit Institute for Bioengineering and Bioscience, Georgia Institute of Technology, Atlanta, GA, USA

[3]Coulter Department of Biomedical Engineering, Georgia Institute of Technology, Atlanta, GA, USA

[4]School of Chemical and Biomolecular Engineering, Georgia Institute of Technology, Atlanta, GA, USA

Abstract

The transformative potential of cells as therapeutic agents is being realized in a wide range of applications, from regenerative medicine to cancer therapy to autoimmune disorders. The majority of these therapies require *ex vivo* expansion of the cellular product, often utilizing fetal bovine serum (FBS) in the culture media. However, the impact of residual FBS on immune responses to cell therapies and the resulting cell therapy outcomes remains unclear. Here, we show that hydrogel-delivered FBS elicits a robust type 2 immune response characterized by infiltration of eosinophils and $CD4^+$ T cells. Host secretion of cytokines associated with type 2 immunity, including IL-4, IL-5, and IL-13, is also increased in FBS-containing hydrogels. We demonstrate that the immune response to xenogeneic serum components dominates the local environment and masks the immunomodulatory effects of biomaterial-delivered mesenchymal stromal/stem cells. Importantly, delivery of relatively small amounts of FBS (3.2% by volume) within BMP-2-containing biomaterial constructs dramatically reduces the ability of these constructs to promote *de novo* bone formation in a radial defect model in immunocompetent mice. These results urge caution when interpreting the immunological and tissue repair outcomes in immunocompetent pre-clinical models from cells and biomaterial constructs that have come in contact with xenogeneic serum components.

Keywords

Immune response; Xenogeneic proteins; Bone regeneration; Tissue regeneration; Hydrogel

*Correspondence to: andres.garcia@me.gatech.edu.

Author Contributions

K.E.M. designed and carried out the research and drafted and edited the figures and manuscript; P.P.K. performed the bone defect model experiments and reviewed the manuscript; M.M.C., and R.S.S. performed the research (flow cytometry and Luminex), analyzed the data, and reviewed the manuscript; H.S.T. analyzed the flow cytometry data and reviewed the manuscript; K.E.M and A.J.G. conceptualized the study, analyzed the data, and wrote the paper; A.J.G. supervised and funded the study.

Introduction

Cell-based therapies represent promising strategies for tissue regeneration, particularly in cases where host cells alone are unable to repair the injury due to disease, age, or excessive trauma. In particular, mesenchymal stem/stromal cells (MSCs) are being studied for regeneration of diverse tissues including skeletal muscle, cardiac muscle, bone, and cartilage [1]. As large numbers of transplanted MSCs are required to achieve therapeutic impact, *ex vivo* expansion of the cellular product is necessary [2, 3]. Additionally, to promote the survival, persistence, and regenerative properties of transplanted cells, MSC therapies are frequently delivered in conjunction with biomaterial scaffolds [4]. Furthermore, as a means of improving the maturation and efficacy of cell-biomaterial constructs, biomaterial scaffolds are often pre-seeded with cells and cultured *ex vivo* prior to implantation [5–7].

Most often, both cells and cell-biomaterial constructs are cultured in media supplemented with fetal bovine serum (FBS) [2]. FBS supplementation is practical because it is a cost-effective approach to provide cells in culture with vital nutrients, attachment factors, and growth factors. However, FBS is problematic clinically due to issues with significant batch to batch variability and not meeting the standards of good manufacturing practices (GMP). Furthermore, case reports from cell therapy clinical trials have shown that patients generate antibodies against xenogeneic serum proteins which, in some cases, have been linked to anaphylactic reactions [8, 9]. Additionally, known complications of delivering xenogeneic serum-based therapeutics, like antivenom for snake bites, include acute anaphylactic reactions and serum sickness, an allergy like hypersensitivity reaction [10]. Although serum-free and xeno-free media formulations have been developed for some cell types (e.g. human T cells and human MSCs) [11, 12], these types of media are not readily available for many cell types, especially non-human cells.

Mice are frequently used as pre-clinical *in vivo* models to test the therapeutic safety and efficacy of cell therapies intended to treat human disease. While early MSC regenerative medicine studies focused on the differentiation capacity of human MSCs in immunocompromised/immunodeficient murine models [13], the field has largely moved on to studying MSC promotion of tissue repair through their immunomodulatory effects mediated by MSC secretion of cytokines, chemokines, and subcellular particles (e.g., extracellular vesicles) [14]. This research has necessitated the use of murine MSCs in immunocompetent mice as a proxy for the human system. However, it is unclear whether residual FBS used for murine MSC expansion impacts their therapeutic outcomes or how immune responses to FBS might obscure the interpretation of immunological responses to MSC therapies in immunocompetent mouse models.

The immune system plays a key role in promoting tissue regeneration as various immune cells scavenge debris and dead cells, recruit tissue progenitor cells, and promote vascularization at the site of injury [15]. In particular, type 2 immune responses are thought to drive tissue repair, most notably through the activities of M2 macrophages and $CD4^+$ T helper 2 cells [16]. Xenogeneic decellularized materials, which elicit a well-characterized type 2 immune response, have been shown to improve tissue regeneration in a variety of

tissues [17]. However, data from chronic inflammation models show that type 2 immunity can be fibrotic, negatively impacting organ repair [18].

Here, we characterized the *in vivo* immune responses to FBS-containing media when delivered subcutaneously within a synthetic hydrogel. Results demonstrate that xenogeneic serum components induce a robust type 2 immune response characterized by infiltration of eosinophils and $CD4^+$ T cells and increased concentrations of type 2 immunity-associated cytokines, including IL-4, IL-5, and IL-13. This FBS-induced immune response masks some features of the *in vivo* immune response to hydrogel-delivered MSCs. Additionally, the FBS-associated immune response impairs biomaterial-directed bone repair outcomes in a murine radial segmental defect model. Thus, FBS from cell culture media may confound interpretation of immunological responses to cell therapies and impede tissue regeneration in pre-clinical models.

Methods

PEG hydrogel synthesis

Hydrogels were prepared by mixing 20 kDa 4-arm poly(ethylene glycol)-maleimide (PEG-4MAL) macromer (Laysan Bio, >95% purity) with the adhesive peptide GRGDSPC (RGD) (GenScript, >95% purity) and the crosslinker GCRDVPMS↓MRGGDRCG (VPM) (Genscript, >95% purity). Hydrogels were synthesized to obtain a final concentration of 1.0 mM RGD and 4% w/v PEG-4MAL. The concentration of crosslinker used for the synthesis of each hydrogel was calculated stoichiometrically by balancing the number of free thiols on the crosslinker with the number of unreacted maleimide groups on the PEG-4MAL following functionalization with RGD. PEG-4MAL, RGD, and VPM were dissolved, individually, in 25 mM HEPES in PBS and the pH of the solutions were adjusted to 4.0 to prevent gelling in the syringe prior to injection (hydrogels polymerize *in situ*). Hydrogels were mixed at a volume ratio of 2:1:1:1 of PEG-4MAL: RGD: VPM: media or cell suspension. Unless otherwise noted, the media portion of the hydrogel was made up of RPMI 1640 (Gibco, 11875093) supplemented with 16% v/v serum, making the final concentration of serum in the hydrogels 3.2%. As controls the media portion was substituted with RPMI 1640 without serum, CellCor CD MSC serum-free, chemically defined media (Xcell, YSP001), or PBS. Murine MSCs (mMSCs) were delivered at a dose of 2.5×10^5 mMSCs per 50 μL PEG-4MAL hydrogel.

Subcutaneous dorsal hydrogel injection

All animal experiments were performed with approval of Georgia Tech Animal Care and Use Committee with veterinary supervision and within the guidelines of the Guide for the Care and Use of Laboratory Animals. Subcutaneous injection studies were carried out as previously described [19]. Briefly, C57BL/6J wild-type mice (8–10 weeks old, Jackson Laboratories) were anesthetized under isoflurane, fur was removed from the dorsal region, and the skin was treated with 70% isopropyl alcohol and chlorohexidine. 50 μL of PEG-4MAL hydrogel solution was mixed in an Eppendorf tube on ice and then injected into the dorsal region of the mouse using a 29½ gauge insulin syringe (Exel, 26018). For experiments with four or fewer conditions, all conditions were injected into individual dorsal

quadrants (randomized) in the same animal to reduce variability due to inherent biological differences across animals.

Flow cytometry of infiltrating immune populations

Hydrogels were explanted for flow cytometry analysis 7 days after injection. Following euthanasia, a midline incision was made the length of the mouse spine, followed by perpendicular incisions to expose the hydrogel samples, which adhere to the subcutaneous side of the skin layer upon polymerization *in situ*. Skin and hydrogels were peeled back, and a 12 mm biopsy punch was used to excise the complete hydrogel sample and the overlying skin. Samples were then placed in 1.0 mL of hydrogel/tissue dissociation buffer (RPMI 1640, 2.5 U/mL Dispase II (ThermoFisher, 17105041), 0.2% Type II Collagenase (Worthington Biochemical Corp., LS004176)), finely cut using scissors, and incubated for 1 h at 37°C. The digested hydrogel/skin solution was then passed through a 35 μm cell strainer (Falcon, 352235) and washed with 5 mL of PBS. Red blood cells were lysed using RBC Lysis Buffer (BioLegend, 420301) and the cell pellet was rinsed first with FACS buffer (HBSS (ThermoFisher, 14175103), 2mM EDTA (Invitrogen, AM9260G), 0.5% BSA (Sigma-Aldrich, A9418)) then with PBS. Cells were stained with Zombie Violet (BioLegend, 423114) for 15 min, washed with FACS buffer, and blocked with TruStain FcX PLUS (BioLegend, 156604) prior to staining with the myeloid, lymphoid, or ILC2 flow panel antibodies for 1 h. FMOs (fluorescence minus one) were run with every acquisition. Cells were fixed using Fixation Buffer (BioLegend, 420801) following manufacturer instructions. Absolute cell counts were calculated on the basis of Precision Count Beads (BioLegend, 424902). Data was collected using a BD FACSAria III flow cytometer and analyzed using FCS Express 7 (De Novo Software). Gating strategies for the three panels are presented in Supplementary Figure 1. FMOs were used to gate the following markers: CD11c, F4/80, MHC-II, CD163, CD86, CD206, CD11b in lymphoid panel, CD4, CD8a, NK1.1, CD19, Lin, ICOS, CD90.2, and ST2.

Luminex multiplex ELISAs

Seven days following injection, hydrogels were explanted for chemokine and cytokine analysis following the same explantation procedure as for flow cytometry analysis. Hydrogel/skin explants were weighed and placed in protein extraction buffer (RIPA Buffer (Sigma, R0278), Protease Inhibitor Cocktail (Sigma, P8340)) at 250 mg/mL on ice. Samples were homogenized by sonication, on ice, in 5 sec intervals at 70% amplitude until hydrogels were well digested. Samples were centrifuged at 10,000xg for 30 min at 4°C, and supernatants were collected, snap frozen, and stored at −80°C until analysis. Samples were analyzed using a Milliplex Mouse Cytokine/Chemokine Magnetic Bead Panel – Premixed 32 Plex (Millipore, MCYTOMAG-70K) or a custom R&D Luminex kit containing the analytes IFNγ, IL-13, IL-17A, IL-25, and IL-33 (R&D, LXSAMSM-05) on a MAGPIX System (Luminex Corp.) according to manufacturer instructions. Analyte concentrations (pg/mL) were calculated from best fit curves generated by the Milliplex Analyst Software (Luminex Corp.). Values for individual samples above/below the analyte detection limit, as determined by the Milliplex Analyst Software, were taken at the maximum/minimum detection value for further analysis. Analytes with the majority of samples out of range for all groups were excluded from further analysis and were reported as either above or below

the limit of detection. Hierarchical clustering (Ward's method, Euclidean distances) and principal-component analysis (unit variance scaling, SVD with imputation) were performed using ClustVis (https://biit.cs.ut.ee/clustvis/) [20].

mMSC isolation, culture, and immunodepletion

Bone marrow was isolated from mouse femurs and tibias as previously described [21]. Red blood cells were lysed using RBC Lysis Buffer (BioLegend, 420301) and the bone marrow cells were then washed with mMSC complete media (RPMI 1640, 16% MSC qualified FBS (Gibco, 12662029), 2 mM L-glutamine, 100 U/mL pen/strep). Bone marrow cells were cultured following a protocol adapted from Caroti et al [22]. Cells were plated at ~250,000 cells/cm^2 in a 15 cm plate in mMSC media supplemented with 10 ng/mL bFGF (Austral Biologicals, GF-030–5) and cultured overnight at 37°C, 5% O_2, 5% CO_2 (hypoxic conditions). After 24 h, non-adherent cells were aspirated, and media was replaced with fresh mMSC media containing 10 ng/mL bFGF. Media was changed every 3–4 days. Cells were passaged for the first time and depleted of immune cells when they reached 90–95% confluence. Immune cell depletion was done by MACS separation using CD45 MicroBeads, mouse (Miltenyi Biotec, 130-052-301) and LD columns (Miltenyi Biotec, 130-042-901). Immune cell-depleted mMSCs were plated at ~2000 cells/cm^2 in a 15 cm plate in mMSC media containing 10 ng/mL bFGF. Media was changed every 3–4 days and cells were passaged at 80% confluence. For all experiments, cells were used between passages 2 and 4.

ELISAs for FBS components bovine BSA, APOA1, and APOB

mMSCs were isolated, cultured, and immunodepleted as described above. Once grown to confluence, cells were trypsinized, washed once with mMSC complete media, and pelleted by centrifugation. mMSCs were then washed either once or 3 times with 15 mL of PBS, centrifuging and aspirating buffer each time. After the final wash, mMSCs were resuspended in 500 μL of PBS and pelleted one final time. ELISAs were run on the supernatant. Supernatant from unwashed mMSCs in mMSC complete media and mMSC complete media without cell were included as positive controls. ELISAs for BSA (Cygnus, F030), bovine APOA1 (LSBio, LS-F54098), and bovine APOB (LSBio, LS-F25212) were run according to manufacturer instructions. Absorbance was read using a Biotek Synergy H4 multi-mode plate reader and analysis was done using Gen5 Data Analysis Software (Biotek).

Bone implant preparation

Implant hydrogels (4.0% w/v 20 kDa PEG-4MAL, 1.0 mM GFOGER adhesive peptide (Aapptec), VPM crosslinker) were synthesized as described above and cast in a polyimide tube with 300 μm laser machined holes (MicroLumen) to improve cellular invasion and nutrient transport into the bone defect site. Hydrogels contained 50 ng BMP-2 (R&D, 355-BM). Half of the samples were synthesized using RPMI 1640 media supplemented with 16% FBS as the buffer component for the media/cell suspension fraction of the hydrogel (final FBS concentration of 3.2% v/v in the hydrogel as a whole). The other half were synthesized using PBS as the buffer component for the media/cell suspension fraction. Implants were cut into 4 mm segments using custom implant cutters. All implants were made within an hour of their implantation in a mouse and stored in the same buffer as their media/cell suspension buffer component prior to implantation to prevent drying out.

Radial segmental defect surgery

All animal experiments were performed with the approval of the Georgia Tech Animal Care and Use Committee with veterinary supervision and within the guidelines of the Guide for the Care and Use of Laboratory Animals. A critically sized bone defect in the mouse radius was used to evaluate bone formation as previously described [23, 24]. C57BL/6J wild-type male mice (8–10 weeks old, Jackson Laboratories) were anesthetized under isoflurane, and fur was removed from the right forelimb. Prior to surgery, mice were given a single dose of slow-release buprenorphine (1 mg/kg) for pain relief, and the right forelimb was disinfected with 70% isopropyl alcohol and chlorohexidine. A 1 cm incision was made on the right limb over the radius, followed by blunt dissection of the radius. Using custom bone cutters, a 2.5 mm defect was made in the right radius, leaving the right ulna intact to stabilize the injury. A 4 mm long polyimide tube containing the implant hydrogel was then fitted over each end of the radius and the overlying incision was closed using Vicryl sutures. Mice were monitored post-surgery for lethargy, weight loss, normal eating habits, and signs of distress.

Live animal uCT

In vivo microCT imaging was performed on anesthetized mice using a VivaCT imaging system (Scanco Medical). A 3.2 mm long section centered over the radial defect was imaged using the following imaging parameters: intensity, 145 μA; energy, 55 kVp; integration time, 200 ms; resolution, 15 μm. De novo bone formation was evaluated by drawing a contour around the radius on each 2D slice and applying a Gaussian filter. The middle 2.0 mm of the defect was identified and analyzed for bone volume, so that only *de novo* bone formation was measured. 3D reconstructed images show the full 3.2 mm length of scanned bone.

Statistics

Statistical analysis was performed using GraphPad Prism 8 (GraphPad Software Inc., La Jolla, CA). Statistical tests and P values are reported in the figure captions of the corresponding figures. For flow cytometry analysis of *in vivo* gels, cell counts were log transformed and a one-way ANOVA was used to detect statistical differences. Where appropriate (all groups were present in all animals), a one-way repeated measures ANOVA was performed to compare inter-subject variables. Tukey's multiple comparisons test with adjustment for multiple comparisons was used to determine differences between specific groups. Multiple comparisons were run on all possible pairings of groups (e.g. FBS vs. RPMI, FBS vs. PBS, RMPI vs. PBS, etc.). For the Luminex data, a one-way ANOVA was used to detect statistical differences followed by Tukey's multiple comparisons test for IL-4, Eotaxin, IL-9, IL-25, and IL-33. For all other cytokines, a Kruskal-Wallis test was used followed by Dunn's multiple comparison test due to the repeated values at the limit of detection for these cytokines. P values are always denoted: *$p<0.05$, **$p<0.01$, ***$p<0.001$, ****$p<0.0001$. Replicates indicated are biological replicates. All data is plotted as mean ± SEM.

Results

FBS alters immune cell infiltration into hydrogels implanted subcutaneously

To evaluate immune responses to FBS in C57BL/6J immunocompetent mice, we first characterized the profile of immune cell infiltration into subcutaneously injected synthetic PEG-4MAL hydrogels synthesized using FBS-containing media as the buffer. PEG-4MAL hydrogels have significant advantages for regenerative medicine applications because of their intrinsic low fouling properties, minimal inflammatory profile *in vivo*, ease in incorporating various bioactive functionalities to promote tissue repair, and ability to be delivered via injection, which minimizes further tissue trauma upon therapeutic delivery [23, 25, 26]. Additionally, by delivering the FBS-containing media in PEG-4MAL hydrogels, we were able to localize the immune response to the hydrogel and immediate surrounding tissues, allowing us to deliver FBS-containing gels and control gels in the same mouse, one gel per each dorsal quadrant [21].

We evaluated the effect of delivery of multiple experimental groups in the same animal by injecting PEG-4MAL hydrogels containing either PBS or 250k mMSCs in 3.2% MSC-qualified FBS in the dorsal subcutaneous space of mice. Mice were split into 3 groups in which: (1) both gels injected contained PBS, (2) both gels injected contained mMSCs in FBS, (3) one gel of each condition were delivered (Supplementary Fig. 2a). On day 14 post-injection, hydrogels were explanted and the infiltrating myeloid populations were evaluated (Supplementary Fig. 2b, c). The ability of the assay to detect differences between groups was maintained in mice where one gel of each group was delivered. However, the assay sensitivity was reduced compared to animals injected with only one group, likely due to immunological cross talk between the different dorsal quadrants. To combat this reduced sensitivity, we increased the number of mice per group in the rest of our studies. For more nuanced immunological studies, it would be pertinent to use separate animals to ensure that no sample cross-contamination has occurred. Additionally, it is impossible to study the systemic consequences of FBS delivery using this model, as individual animals per group would be required. However, given the stark contrast in immune responses between our treatment groups which allowed us to detect statistically significant differences in broadly defined immune populations in the co-delivery model, we chose to proceed with this model as it significantly reduces biological variability within studies.

In all studies, hydrogels were synthesized in volume ratios of 2:1:1:1 PEG-4MAL macromer solution: VPM cross-linker solution: RGD adhesive ligand solution: cell suspension/cell-free media. The media portion of the hydrogels in these studies consisted of RPMI 1640 supplemented with 16% v/v serum (based on our typical MSC media formulation), making the final concentration of serum in the hydrogels 3.2%. The following groups were studied: RPMI 1640 media + 16% FBS (FBS), RPMI 1640 alone (RPMI), Xcell Chemically-Defined media (CD), and phosphate buffered saline (PBS) (Fig. 1a). The FBS used in these studies is MSC-qualified FBS, screened to support the *in vitro* expansion and clonal enumeration of MSCs. CD is a commercially available media formulation in which the serum component is replaced with a proprietary combination of recombinant proteins specifically designed for the *in vitro* expansion of human MSCs (no such equivalent formulation is available for

murine MSCs; murine MSCs do not grow in this media formulation). To form the hydrogels, a mixture of all components was injected into subcutaneous space in the mouse dorsum and the gel was allowed to polymerize *in situ*.

On day 7 post-injection, hydrogels were explanted, digested to obtain infiltrating immune cells, and analyzed by multiparametric flow cytometry using validated gating strategies (Supplementary Fig. 1). We found that hydrogels containing FBS injected in the subcutaneous space elicited an immune response distinct from those containing RPMI, CD, or PBS, and there were no differences in immune cells among hydrogels containing RPMI, CD, and PBS (Fig. 1b–f). Cell counts reported are per 50 μL hydrogel explant and are not normalized as the weight of the hydrogel explants is consistent across experimental conditions (Supplementary Fig. 3). There were notable changes in the profile of infiltrating cells in both the myeloid and lymphoid compartments (Fig. 1b, c). Specifically, in the myeloid compartment, the numbers of infiltrating Siglec-F^+ eosinophils, $Ly6C^{hi}$ monocytes, and $ICOS^+CD90.2^+ST2^+$ type 2 innate lymphoid cells (ILC2s) were significantly increased in hydrogels containing FBS compared to the other three conditions (Fig. 1d, e). Additionally, we observed significant increases in the number of NKT cells, $CD4^+$ T cells, and $CD8^+$ T cells in FBS-containing hydrogels (Fig. 1f). We did not observe any significant differences in the number of other infiltrating immune cell populations between FBS- and PBS-containing hydrogels; however, there was an increase in the number of B cells in FBS containing gels compared to RPMI gels and CD gels and an increase in the number of NK cells in FBS containing gels compared to RPMI gels (Supplementary Fig. 4). There was no discernable dermatitis observed at the day 7 time point for any experimental group.

FBS-containing hydrogels drive local increases in type 2 immunity-associated cytokines

To further characterize the immune response to FBS-containing hydrogels, we analyzed the day 7 murine cytokine milieu within subcutaneous media-containing hydrogels via a Luminex multiplexed bead-based ELISA. Hierarchical clustering analysis of the cytokine milieu shows that the FBS group clusters distinctly from the control groups by a cytokine profile that is dominated by IL-7, IL-12, GM-CSF, IL-13, IL-5, IL-3, Il-2, Eotaxin, and IL-4 (Fig. 2a). Principal component analysis (PCA) similarly results in hydrogels containing FBS clustering distinctly from the other three conditions (Fig. 2b). We also observed differential production of many individual cytokines classically associated with type 2 immune responses to parasites and allergens, including IL-3, IL-4, IL-5, IL-10, IL-13, Eotaxin, and GM-CSF (Fig. 2c) [27, 28]. Interestingly, other type 2-associated cytokines IL-9 and the alarmins IL-25 and IL-33 showed no differences among groups (Fig. 2c). Alarmins are thought to be secreted by epithelial and stromal cells upon exposure to parasites or allergens, activating ILC2 production of IL-5 and IL-13 and initiating the type 2 immune response [29–31], so it is notable that differences in alarmin secretion between groups are absent, although this may be due to the relatively late time point studied.

Other cytokines differentially regulated by hydrogels containing FBS include IL-2, IL-7, and IL-12p40 (Fig. 2c). IL-2 and IL-7 are both key T cell cytokines. IL-2 has been shown to play a role in $CD4^+$ T helper 2 cell (Th2) and regulatory T cell (Treg) differentiation and

function [32, 33], while IL-7 is often associated with the generation of $CD4^+$ memory T cells [34, 35]. IL-12 is an important driver of type 1 immune responses, playing an essential role in $CD4^+$ T helper 1 cell (Th1) development and inducing IFNγ production [36], while inhibiting the development of IL-4 producing Th2 cells [37]. This increase in IL-12 may indicate the beginning of some sort of regulatory negative feedback mechanism; however, TNFα and IFNγ, other type 1 immunity-associated cytokines, showed no differences in concentration among groups. Type 3 immunity-associated cytokine IL-17A was below the limit of detection in all groups at the day 7 time point [38]. All other cytokines assayed also showed no differences among groups (Supplementary Fig. 5). There were no differences in any cytokines among the control groups: RPMI, CD, and PBS.

Taken together, the immune profiling by flow cytometry and multiplexed ELISA demonstrates that hydrogels containing FBS, when delivered subcutaneously in a C57BL/6J mouse, induce a robust type 2 immune response characterized by infiltration of eosinophils, ILC2s, and $CD4^+$ helper T cells. Additionally, the local cytokine response to FBS-containing hydrogels is dominated by type 2 immunity-associated cytokines with minimal differences in cytokines associated with type 1 or type 3 immunity.

Immune response induced by FBS-containing gel is specific to xenogeneic serum

We next assessed whether this immune response to FBS-containing hydrogels is specific to one lot of FBS, xenogeneic serum, or serum in general. To this end, we compared the immune responses to six different types of serum. We analyzed three different types of FBS: (1) MSC qualified-FBS, as used in the preceding studies, (2) heat-inactivated FBS, as complement that is not denatured by heat can cause an immune response, and (3) Hyclone FBS, which was screened to not activate T cells *in vitro*. We also analyzed porcine serum (xenogeneic in mice), BALB/c mouse serum (allogeneic in C57BL/6J mice), and C57BL/6J mouse serum (autologous in C57BL/6J mice). PBS was used as a negative control.

For all three types of FBS and porcine serum (PorS) delivered with hydrogels, we saw a significant increase in the amounts of infiltrating eosinophils and $CD4^+$ T cells compared to the two types of mouse serum and PBS (Fig. 3a). There were also differences in the number of infiltrating DCs, CD8 T cells, and NKT cells between FBS/porcine serum and mouse serum/PBS and no differences between the other immune populations analyzed (Supplementary Fig. 6). Notably, there was no significant difference in the number of infiltrating immune cell populations between gels containing either BALB/c or C57BL/6J mouse serum and PBS, indicating that delivery of murine serum components does not initiate a type 2 immune response (Fig. 3a). Type 2 immune responses have previously been reported in response to other sources of xenogeneic proteins, especially xenogeneic decellularized extracellular matrices (ECM) [39–41]. Collectively, this data indicates that the type 2 immune response elicited by FBS-containing hydrogels is a reaction specific to xenogeneic serum components.

Macrophage phenotype shifts in response to xenogeneic serum

Since type 2 immune responses are associated with an alternatively activated, M2 macrophage phenotype [27], we assessed the number and phenotype of macrophages

infiltrating FBS- and porcine serum-containing hydrogels compared to gels containing mouse serum or PBS. There was no difference in the number of infiltrating $F4/80^+$ macrophages among groups (Fig. 3a). M2 macrophages are often identified by increased expression of M2 marker CD206 and decreased expression of M1 marker CD86 [42]. Interestingly, we saw no differences in CD206 or CD86 expression between the FBS/porcine serum groups and the mouse serum/PBS groups (Fig. 3b–d). There was, however, an increase in the proportion of $CD206^+CD163^+$ double positive macrophages in the FBS- and porcine serum-containing hydrogel groups compared to controls, with the vast majority of the $CD163^+$ population co-expressing CD206 (Fig. 3b–d). Macrophage MHC-II expression was also increased in FBS- and porcine serum-containing hydrogels. $CD206^+CD163^+$ double positive macrophages are typically considered to be a subtype of M2 macrophages [42], whereas macrophage expression of MHC-II indicates that those macrophages are involved in antigen presentation [43]. The presence of these two phenotypes of macrophages in xenogeneic serum-containing gels is again consistent with prior literature, where xenogeneic porcine decellularized ECM is associated with two distinct macrophage populations, one $CD301b^+CD206^{hi}CD163^+$ and the other $CD9^+CD301b^+MHC\text{-}II^{hi}$ [44].

Immune response to FBS-containing hydrogels masks mMSC immunomodulatory effects

Due to their potent immunomodulatory and trophic properties, MSCs are being evaluated as a therapy in a wide range of inflammatory diseases as well as for their potential in promoting tissue regeneration [1]. We thus sought to explore the impact FBS has on the immune response to murine MSC (mMSC)-containing hydrogels in an *in vivo* setting. Neither Xcell Chemically-Defined media, intended for the culture of human MSCs, nor media supplemented with mouse serum supported the *ex vivo* expansion of mMSCs in our hands (Supplementary Fig. 7). Therefore, we isolated bone marrow from mouse femora and tibiae and expanded the isolated mMSCs in media supplemented with FBS (Fig. 4a). mMSC phenotype and purity were confirmed by flow cytometry for MSC surface marker expression (Supplementary Fig. 8). To minimize the amount of FBS delivered with the mMSCs, the cell pellet was thoroughly washed, either once or 3 times with 15 mL of PBS, prior to delivery. To evaluate the reduction in serum components present in the cell suspension following washing, we measured the concentration of serum proteins bovine serum albumin (BSA), bovine apolipoprotein A1 (APOA1), and bovine apolipoprotein B (APOB) by ELISA (Fig. 4b, Supplementary Fig. 9a). These proteins constitute a large portion of all proteins in FBS and are suggested negative markers for FBS contamination by the International Society for Extracellular Vesicles [45]. Washing the mMSC cell pellet three times with PBS resulted in a 100-fold decrease in BSA, a 100-fold decrease in APOA1 and a 1000-fold decrease in APOB concentrations (Fig. 4b, Supplementary Fig. 9a).

To study the *in vivo* effects of FBS on the immune response to mMSC-laden hydrogels, PEG-4MAL hydrogels containing 2.5×10^5 mMSCs washed 3 times with either FBS-containing media or PBS were injected into the dorsal quadrants of C57BL/6J mice. Cell-free hydrogels containing either 3.2% FBS or PBS were included as references. Similar trends in immune cell infiltration were observed between cell-free and mMSC-laden FBS and PBS containing gels (Fig. 4c, d, Supplementary Fig. 9b). This is especially notable for the infiltration of the type 2 immune response-associated cell populations, eosinophils

and $CD4^+$ T cells. Strikingly, washing the mMSC cell pellet resulted in a dramatic drop in these populations to levels no different from cell-free PBS gels, indicating that the dominant immune response was to FBS and not the mMSCs (Fig. 4c, d).

The neutrophil response is the exception, where the presence of mMSCs, with or without FBS, decreases the number of infiltrating neutrophils compared to cell-free FBS-containing gels (Fig. 4c). This is consistent with previous studies that demonstrate that an important mechanism through which MSCs modulate inflammatory responses is by suppressing neutrophil activation and inhibiting neutrophil migration [46–48]. Additionally, we observed that gels containing washed mMSCs contain fewer $Ly6C^{hi}$ monocytes than PBS control gels (Fig. 4c), which again agrees with previous studies reporting MSC inhibition of $Ly6C^{hi}$ monocyte recruitment and promotion of a $Ly6C^{hi}$ to $Ly6C^{lo}$ monocyte phenotypic shift at sites of inflammation [48, 49]. This neutrophil and monocyte data indicates that the mMSCs delivered in our experiments are active and being delivered at a high enough dose to elicit an immunological response, however the presence of FBS masks these responses in some instances. Taken together, this shows that washing mMSCs in PBS prior to injection mitigates the dominant FBS immune response and allows for mMSC immunomodulation to be discriminated from the FBS-induced immune response.

Delivery of FBS within biomaterial-based bone repair constructs reduces de novo bone formation

As FBS clearly elicits a strong immune response, we next assess the impact this immune response has on biomaterial-directed tissue repair. We have previously shown that delivery of the osteogenic protein BMP-2 within PEG-4MAL hydrogels presenting the adhesive ligand GFOGER robustly regenerates bone in an immunocompetent (C57BL/6J) mouse model [24]. We, thus, focused on biomaterial/BMP-2-directed bone regeneration as the impact of FBS co-delivery on BMP-2 induced regeneration is easier to interpret than co-delivery of MSCs and FBS. This is because MSCs are posited to have potent immunomodulatory and regenerative properties that could confound interpretation of the effect of FBS on the host [50].

To explore the effect of FBS on biomaterial-directed bone regeneration, GFOGER-functionalized PEG-4MAL hydrogel constructs containing 50 ng BMP-2, with or without 3.2% FBS by volume in the buffer, were cast within 4 mm polyimide tubes (Fig. 5a). These constructs were then implanted into 2.5 mm-long unilateral critical-sized radial defects and *de novo* bone formation was assessed 4 weeks post-surgery by micro-computed tomography (μCT). Our results demonstrate that the presence of FBS significantly reduces the ability of BMP-2-containing biomaterial constructs to form new bone (Fig. 5b, c).

Discussion

In this study, we demonstrate that the type 2 immune response elicited by xenogeneic serum delivered within a synthetic PEG-4MAL hydrogel masks the effects of MSC immunomodulation in an *in vivo* setting and impairs biomaterial-directed BMP-2 bone repair. Type 2 immune responses are characterized by the production of cytokines IL-4, IL-5, and IL-13 [27]. Numerous disparate stimuli evoke a classical type 2 response,

including parasites (e.g. helminths), allergens, and extracellular bacteria [18]. In addition, many of the key cell types associated with type 2 immune responses, including $CD4^+$ T helper 2 cells (Th2s), eosinophils, mast cells, basophils, type 2 innate lymphoid cells (ILC2s), and IL-4- and IL-13-activated M2 macrophages, have been implicated in various tissue repair and fibrotic processes [18]. Induction of this response by xenogeneic proteins, however, remains much less studied.

Xenogeneic decellularized extracellular matrix (ECM)-derived materials are being explored for use in regenerative medicine [51]. These ECM-derived materials contain an ill-defined mixture of proteins, proteoglycans, matrix-bound vesicles, and other molecules that together have been shown to elicit a strong type 2 immune response [39, 41, 52]. Our results indicate that xenogeneic, but not allogeneic, serum components localized within synthetic hydrogels promote similar type 2 immune responses in an immunocompetent mouse model. This result is consistent with studies of ECM-derived materials in both wild-type and humanized mouse models where xenogeneic, but not allogeneic, materials were shown to promote a Th2-restricted, type 2 immune response [40, 53, 54]. Other biologically-sourced materials that are not synthesized endogenously in mice also elicit type 2 immune responses, including chitin [55, 56], helminth egg derivatives [57], and materials crosslinked with D-chiral peptides [58], which suggests a broader mechanism of xenogeneic protein recognition by type 2 immune cells. Granted, there is substantial heterogeneity in the signals which initiate type 2 immune responses, and which molecules are being recognized by which cells largely remains an outstanding question in the field of type 2 immunity [30, 31].

Although we show that the robust type 2 immune response to FBS impedes tissue regeneration in a bone repair model, others, including most reports studying ECM-derived materials, allude to this immune response being pro-regenerative [17]. In fact, type 2 immunity is rather Janus-faced. In previous studies of acute injury, eosinophil depletion and knock out of type 2 immune response associated cytokines have been shown to impair liver and skeletal muscle repair in murine models [59, 60]. However, in chronic inflammatory conditions, such as non-alcoholic steatohepatitis (NASH) [61], Duchenne muscular dystrophy (DMD) [62], and chronic pulmonary disease [63], high levels of type 2 cytokines and eosinophilia are frequently associated with increased fibrosis. Additionally, the type 2 immune response associated with wear debris from prosthetic joints was recently shown to result in fibrosis, loss of cartilaginous and osseous tissues, and joint implant failure in humans [30, 64]. Indeed, in many studies specifically looking at M2 macrophages, efficient healing is dependent on a finely tuned timing, duration, and magnitude of the M2 response [42]. Appropriate regulation of the M2 response leads to successful tissue repair whereas chronic type 2 inflammation leads to exaggerated repair mechanisms, including uncontrolled myofibroblast differentiation and activation and excessive collagen deposition, which ultimately leads to fibrosis [42]. More research is needed to better understand the mechanisms driving these dichotomous outcomes of type 2 immune responses.

Our study indicates that rigorous washing protocols for cell products can mitigate xenogeneic serum induced immune responses at a day 7 time point. It is important, however, to note that serum components may be internalized by cells, for example serum component-enriched biomolecular coronas on nanoparticles promote their uptake by cells [65, 66], and

these internalized serum components could still lead to immunogenicity. Additionally, it takes the adaptive immune system 1–2 weeks to mount a response to a new antigen, so the strength of the adaptive immune response may continue to grow with time past the day 7 time point used in this study. Humoral immunity could also play a role in the immune response to xenogeneic serum. Host humoral immune responses to xenogeneic materials in humans are often initiated by antibodies against the cell surface epitope galactose-alpha 1–3-galactose (α-gal), a sugar found in all mammals except old world monkeys, apes, and humans [17, 67]. Antibodies are also formed against non-α-gal antigens, as humoral immune responses are mounted against unknown xenogeneic antigens in tissues derived from α-gal knockout animals [68, 69]. Furthermore, it is unclear how much residual antigen is tolerable, making thorough washing an imperfect solution. Development of more broadly usable, serum-free media alternatives would be ideal.

Cell-biomaterial constructs remain a promising strategy for regenerating injured and diseased tissues. To translate these therapies to the clinic, immune responses to these constructs need to be considered. Going forward, it will be important to account for the impact of reagents used for *ex vivo* manipulation of cells and cell-biomaterial constructs when evaluating immune responses in pre-clinical models.

Supplementary Material

Refer to Web version on PubMed Central for supplementary material.

Acknowledgements

The authors acknowledge funding from the National Institute of Arthritis and Musculoskeletal and Skin Diseases of the National Institutes of Health (R01AR062368, R01AR062920 [A.J.G.]), National Science Foundation Graduate Research Fellowships [K.E.M. and R.S.S.]), and a JDRF Postdoctoral Fellowship (3-PDF-2019-743-A-N [M.M.C.]). The content is solely the responsibility of the authors and does not necessarily represent the official views of the National Institutes of Health or National Science Foundation. The authors thank Petit Institute for Bioengineering and Bioscience at the Georgia Institute of Technology core facilities for access and user support of their equipment. The authors also thank Levi Wood for his support and access to lab equipment.

Data Availability

All data files required to reproduce these findings are available from the corresponding author upon reasonable request.

References

[1]. Levy O, Kuai R, Siren EMJ, Bhere D, Milton Y, Nissar N, Biasio MD, Heinelt M, Reeve B, Abdi R, Alturki M, Fallatah M, Almalik A, Alhasan AH, Shah K, Karp JM, Shattering barriers toward clinically meaningful MSC therapies, Science Advances 6(30) (2020) eaba6884. [PubMed: 32832666]

[2]. Lee MS, Youn C, Kim JH, Park BJ, Ahn J, Hong S, Kim YD, Shin YK, Park SG, Enhanced Cell Growth of Adipocyte-Derived Mesenchymal Stem Cells Using Chemically-Defined Serum-Free Media, Int J Mol Sci 18(8) (2017).

[3]. Bieback K, Hecker A, Kocaömer A, Lannert H, Schallmoser K, Strunk D, Klüter H, Human Alternatives to Fetal Bovine Serum for the Expansion of Mesenchymal Stromal Cells from Bone Marrow, STEM CELLS 27(9) (2009) 2331–2341. [PubMed: 19544413]

[4]. De Pieri A, Rochev Y, Zeugolis DI, Scaffold-free cell-based tissue engineering therapies: advances, shortfalls and forecast, npj Regenerative Medicine 6(1) (2021) 18. [PubMed: 33782415]

[5]. Baldwin J, Antille M, Bonda U, De-Juan-Pardo EM, Khosrotehrani K, Ivanovski S, Petcu EB, Hutmacher DW, In vitro pre-vascularisation of tissue-engineered constructs A co-culture perspective, Vasc Cell 6 (2014) 13. [PubMed: 25071932]

[6]. Erickson IE, Kestle SR, Zellars KH, Dodge GR, Burdick JA, Mauck RL, Improved cartilage repair viain vitropre-maturation of MSC-seeded hyaluronic acid hydrogels, Biomedical Materials 7(2) (2012) 024110. [PubMed: 22455999]

[7]. Byers BA, Guldberg RE, García AJ, Synergy between Genetic and Tissue Engineering: Runx2 Overexpression and in Vitro Construct Development Enhance in Vivo Mineralization, Tissue Engineering 10(11–12) (2004) 1757–1766. [PubMed: 15684684]

[8]. Sundin M, Ringdén O, Sundberg B, Nava S, Götherström C, Le Blanc K, No alloantibodies against mesenchymal stromal cells, but presence of anti-fetal calf serum antibodies, after transplantation in allogeneic hematopoietic stem cell recipients, Haematologica 92(9) (2007) 1208–15. [PubMed: 17666368]

[9]. Mackensen A, Dräger R, Schlesier M, Mertelsmann R, Lindemann A, Presence of IgE antibodies to bovine serum albumin in a patient developing anaphylaxis after vaccination with human peptide-pulsed dendritic cells, Cancer Immunol Immunother 49(3) (2000) 152–6. [PubMed: 10881694]

[10]. de Silva HA, Ryan NM, de Silva HJ, Adverse reactions to snake antivenom, and their prevention and treatment, Br J Clin Pharmacol 81(3) (2016) 446–52. [PubMed: 26256124]

[11]. Chase LG, Lakshmipathy U, Solchaga LA, Rao MS, Vemuri MC, A novel serum-free medium for the expansion of human mesenchymal stem cells, Stem Cell Research & Therapy 1(1) (2010) 8. [PubMed: 20504289]

[12]. Smith C, Økern G, Rehan S, Beagley L, Lee SK, Aarvak T, Schjetne KW, Khanna R, Ex vivo expansion of human T cells for adoptive immunotherapy using the novel Xeno-free CTS immune cell serum replacement, Clinical & translational immunology 4(1) (2015) e31. [PubMed: 25671129]

[13]. Hwang NS, Zhang C, Hwang YS, Varghese S, Mesenchymal stem cell differentiation and roles in regenerative medicine, Wiley Interdiscip Rev Syst Biol Med 1(1) (2009) 97–106. [PubMed: 20835984]

[14]. Weiss ARR, Dahlke MH, Immunomodulation by Mesenchymal Stem Cells (MSCs): Mechanisms of Action of Living, Apoptotic, and Dead MSCs, Front Immunol 10 (2019) 1191. [PubMed: 31214172]

[15]. Shanley LC, Mahon OR, Kelly DJ, Dunne A, Harnessing the innate and adaptive immune system for tissue repair and regeneration: Considering more than macrophages, Acta Biomaterialia 133 (2021) 208–221. [PubMed: 33657453]

[16]. Sadtler K, Estrellas K, Allen BW, Wolf MT, Fan H, Tam AJ, Patel CH, Luber BS, Wang H, Wagner KR, Powell JD, Housseau F, Pardoll DM, Elisseeff JH, Developing a pro-regenerative biomaterial scaffold microenvironment requires T helper 2 cells, Science 352(6283) (2016) 366–370. [PubMed: 27081073]

[17]. Yu Y, Zhang W, Liu X, Wang H, Shen J, Xiao H, Mei J, Chai Y, Wen G, Extracellular matrix scaffold-immune microenvironment modulates tissue regeneration, Composites Part B: Engineering 230 (2022) 109524.

[18]. Gieseck RL, Wilson MS, Wynn TA, Type 2 immunity in tissue repair and fibrosis, Nature Reviews Immunology 18(1) (2018) 62–76.

[19]. Schneider RS, Vela AC, Williams EK, Martin KE, Lam WA, García AJ, High-Throughput On-Chip Human Mesenchymal Stromal Cell Potency Prediction, Advanced Healthcare Materials n/a(n/a) (2021) 2101995.

[20]. Metsalu T, Vilo J, ClustVis: a web tool for visualizing clustering of multivariate data using Principal Component Analysis and heatmap, Nucleic Acids Res 43(W1) (2015) W566–70. [PubMed: 25969447]

[21]. Coronel MM, Martin KE, Hunckler MD, Kalelkar P, Shah RM, García AJ, Hydrolytically Degradable Microgels with Tunable Mechanical Properties Modulate the Host Immune Response, Small (2022) 2106896.

[22]. Caroti CM, Ahn H, Salazar HF, Joseph G, Sankar SB, Willett NJ, Wood LB, Taylor WR, Lyle AN, A Novel Technique for Accelerated Culture of Murine Mesenchymal Stem Cells that Allows for Sustained Multipotency, Scientific Reports 7(1) (2017) 13334. [PubMed: 29042571]

[23]. Clark AY, Martin KE, García JR, Johnson CT, Theriault HS, Han WM, Zhou DW, Botchwey EA, García AJ, Integrin-specific hydrogels modulate transplanted human bone marrow-derived mesenchymal stem cell survival, engraftment, and reparative activities, Nature Communications 11(1) (2020) 114.

[24]. Shekaran A, García JR, Clark AY, Kavanaugh TE, Lin AS, Guldberg RE, García AJ, Bone regeneration using an alpha 2 beta 1 integrin-specific hydrogel as a BMP-2 delivery vehicle, Biomaterials 35(21) (2014) 5453–5461. [PubMed: 24726536]

[25]. Cruz-Acuña R, Quirós M, Farkas AE, Dedhia PH, Huang S, Siuda D, García-Hernández V, Miller AJ, Spence JR, Nusrat A, García AJ, Synthetic hydrogels for human intestinal organoid generation and colonic wound repair, Nat Cell Biol 19(11) (2017) 1326–1335. [PubMed: 29058719]

[26]. Phelps EA, Headen DM, Taylor WR, Thulé PM, García AJ, Vasculogenic bio-synthetic hydrogel for enhancement of pancreatic islet engraftment and function in type 1 diabetes, Biomaterials 34(19) (2013) 4602–4611. [PubMed: 23541111]

[27]. Lloyd CM, Snelgrove RJ, Type 2 immunity: Expanding our view, Sci Immunol 3(25) (2018).

[28]. Asquith KL, Ramshaw HS, Hansbro PM, Beagley KW, Lopez AF, Foster PS, The IL-3/IL-5/GM-CSF Common β Receptor Plays a Pivotal Role in the Regulation of Th2 Immunity and Allergic Airway Inflammation, The Journal of Immunology 180(2) (2008) 1199–1206. [PubMed: 18178860]

[29]. Vannella KM, Ramalingam TR, Borthwick LA, Barron L, Hart KM, Thompson RW, Kindrachuk KN, Cheever AW, White S, Budelsky AL, Comeau MR, Smith DE, Wynn TA, Combinatorial targeting of TSLP, IL-25, and IL-33 in type 2 cytokine–driven inflammation and fibrosis, Science Translational Medicine 8(337) (2016) 337ra65–337ra65.

[30]. El-Naccache DW, Haskó G, Gause WC, Early Events Triggering the Initiation of a Type 2 Immune Response, Trends in Immunology 42(2) (2021) 151–164. [PubMed: 33386241]

[31]. Gause WC, Rothlin C, Loke P.n., Heterogeneity in the initiation, development and function of type 2 immunity, Nature Reviews Immunology 20(10) (2020) 603–614.

[32]. Chinen T, Kannan AK, Levine AG, Fan X, Klein U, Zheng Y, Gasteiger G, Feng Y, Fontenot JD, Rudensky AY, An essential role for the IL-2 receptor in Treg cell function, Nature Immunology 17(11) (2016) 1322–1333. [PubMed: 27595233]

[33]. Cote-Sierra J, Foucras G, Guo L, Chiodetti L, Young HA, Hu-Li J, Zhu J, Paul WE, Interleukin 2 plays a central role in Th2 differentiation, Proceedings of the National Academy of Sciences 101(11) (2004) 3880–3885.

[34]. Yeon S.-m., Halim L, Chandele A, Perry CJ, Kim SH, Kim S-U, Byun Y, Yuk SH, Kaech SM, Jung YW, IL-7 plays a critical role for the homeostasis of allergen-specific memory CD4 T cells in the lung and airways, Scientific Reports 7(1) (2017) 11155. [PubMed: 28894184]

[35]. Li J, Huston G, Swain SL IL-7 Promotes the Transition of CD4 Effectors to Persistent Memory Cells, Journal of Experimental Medicine 198(12) (2003) 1807–1815. [PubMed: 14676295]

[36]. Mullen AC, High FA, Hutchins AS, Lee HW, Villarino AV, Livingston DM, Kung AL, Cereb N, Yao T-P, Yang SY, Reiner SL, Role of T-bet in Commitment of TH1 Cells Before IL-12-Dependent Selection, Science 292(5523) (2001) 1907–1910. [PubMed: 11397944]

[37]. Manetti R, Parronchi P, Giudizi MG, Piccinni MP, Maggi E, Trinchieri G, Romagnani S, Natural killer cell stimulatory factor (interleukin 12 [IL-12]) induces T helper type 1 (Th1)-specific immune responses and inhibits the development of IL-4-producing Th cells, Journal of Experimental Medicine 177(4) (1993) 1199–1204. [PubMed: 8096238]

[38]. Annunziato F, Romagnani C, Romagnani S, The 3 major types of innate and adaptive cell-mediated effector immunity, Journal of Allergy and Clinical Immunology 135(3) (2015) 626–635. [PubMed: 25528359]

[39]. Wang X, Chung L, Hooks J, Maestas DR, Lebid A, Andorko JI, Huleihel L, Chin AF, Wolf M, Remlinger NT, Stepp MA, Housseau F, Elisseeff JH, Type 2 immunity induced by bladder extracellular matrix enhances corneal wound healing, Science Advances 7(16) (2021) eabe2635. [PubMed: 33863719]

[40]. Wang RM, Johnson TD, He J, Rong Z, Wong M, Nigam V, Behfar A, Xu Y, Christman KL, Humanized mouse model for assessing the human immune response to xenogeneic and allogeneic decellularized biomaterials, Biomaterials 129 (2017) 98–110. [PubMed: 28334641]

[41]. Han J, Cherry C, Ruta A, Maestas DR, Mejias JC, Nguyen HH, Fertig EJ, Housseau F, Ganguly S, Moore EM, Tam AJ, Pardoll DM, Elisseeff JH, Age-related Immune-Stromal Networks Inhibit Response to Regenerative Immunotherapies, bioRxiv (2021) 2021.08.17.456641.

[42]. Martin KE, García AJ, Macrophage phenotypes in tissue repair and the foreign body response: Implications for biomaterial-based regenerative medicine strategies, Acta Biomater 133 (2021) 4–16. [PubMed: 33775905]

[43]. Randolph GJ, Jakubzick C, Qu C, Antigen presentation by monocytes and monocyte-derived cells, Current Opinion in Immunology 20(1) (2008) 52–60. [PubMed: 18160272]

[44]. Sommerfeld SD, Cherry C, Schwab RM, Chung L, Maestas DR Jr., Laffont P, Stein JE, Tam A, Ganguly S, Housseau F, Taube JM, Pardoll DM, Cahan P, Elisseeff JH, Interleukin-36γ-producing macrophages drive IL-17-mediated fibrosis, Sci Immunol 4(40) (2019).

[45]. Théry C, Witwer KW, Aikawa E, Alcaraz MJ, Anderson JD, Andriantsitohaina R, Antoniou A, Arab T, Archer F, Atkin-Smith GK, Ayre DC, Bach J-M, Bachurski D, Baharvand H, Balaj L, Baldacchino S, Bauer NN, Baxter AA, Bebawy M, Beckham C, Bedina Zavec A, Benmoussa A, Berardi AC, Bergese P, Bielska E, Blenkiron C, Bobis-Wozowicz S, Boilard E, Boireau W, Bongiovanni A, Borràs FE, Bosch S, Boulanger CM, Breakefield X, Breglio AM, Brennan MÁ, Brigstock DR, Brisson A, Broekman MLD, Bromberg JF, Bryl-Górecka P, Buch S, Buck AH, Burger D, Busatto S, Buschmann D, Bussolati B, Buzás EI, Byrd JB, Camussi G, Carter DRF, Caruso S, Chamley LW, Chang Y-T, Chen C, Chen S, Cheng L, Chin AR, Clayton A, Clerici SP, Cocks A, Cocucci E, Coffey RJ, Cordeiro-da-Silva A, Couch Y, Coumans FAW, Coyle B, Crescitelli R, Criado MF, D'Souza-Schorey C, Das S, Datta Chaudhuri A, de Candia P, De Santana EF, De Wever O, del Portillo HA, Demaret T, Deville S, Devitt A, Dhondt B, Di Vizio D, Dieterich LC, Dolo V, Dominguez Rubio AP, Dominici M, Dourado MR, Driedonks TAP, Duarte FV, Duncan HM, Eichenberger RM, Ekström K, El Andaloussi S, Elie-Caille C, Erdbrügger U, Falcón-Pérez JM, Fatima F, Fish JE, Flores-Bellver M, Försönits A, Frelet-Barrand A, Fricke F, Fuhrmann G, Gabrielsson S, Gámez-Valero A, Gardiner C, Gärtner K, Gaudin R, Gho YS, Giebel B, Gilbert C, Gimona M, Giusti I, Goberdhan DCI, Görgens A, Gorski SM, Greening DW, Gross JC, Gualerzi A, Gupta GN, Gustafson D, Handberg A, Haraszti RA, Harrison P, Hegyesi H, Hendrix A, Hill AF, Hochberg FH, Hoffmann KF, Holder B, Holthofer H, Hosseinkhani B, Hu G, Huang Y, Huber V, Hunt S, Ibrahim AG-E, Ikezu T, Inal JM, Isin M, Ivanova A, Jackson HK, Jacobsen S, Jay SM, Jayachandran M, Jenster G, Jiang L, Johnson SM, Jones JC, Jong A, Jovanovic-Talisman T, Jung S, Kalluri R, Kano S.-i., Kaur S, Kawamura Y, Keller ET, Khamari D, Khomyakova E, Khvorova A, Kierulf P, Kim KP, Kislinger T, Klingeborn M, Klinke DJ, Kornek M, Kosanović MM, Kovács ÁF, Krämer-Albers E-M, Krasemann S, Krause M, Kurochkin IV, Kusuma GD, Kuypers S, Laitinen S, Langevin SM, Languino LR, Lannigan J, Lässer C, Laurent LC, Lavieu G, Lázaro-Ibáñez E, Le Lay S, Lee M-S, Lee YXF, Lemos DS, Lenassi M, Leszczynska A, Li ITS, Liao K, Libregts SF, Ligeti E, Lim R, Lim SK, Linē A, Linnemannstöns K, Llorente A, Lombard CA, Lorenowicz MJ, Lörincz ÁM, Lötvall J, Lovett J, Lowry MC, Loyer X, Lu Q, Lukomska B, Lunavat TR, Maas SLN, Malhi H, Marcilla A, Mariani J, Mariscal J, Martens-Uzunova ES, Martin-Jaular L, Martinez MC, Martins VR, Mathieu M, Mathivanan S, Maugeri M, McGinnis LK, McVey MJ, Meckes DG, Meehan KL, Mertens I, Minciacchi VR, Möller A, Møller Jørgensen M, Morales-Kastresana A, Morhayim J, Mullier F, Muraca M, Musante L, Mussack V, Muth DC, Myburgh KH, Najrana T, Nawaz M, Nazarenko I, Nejsum P, Neri C, Neri T, Nieuwland R, Nimrichter L, Nolan JP, Nolte-'t Hoen ENM, Noren Hooten N, O'Driscoll L, O'Grady T, O'Loghlen A, Ochiya T, Olivier M, Ortiz A, Ortiz LA, Osteikoetxea X, Østergaard O, Ostrowski M, Park J, Pegtel DM, Peinado H, Perut F, Pfaffl MW, Phinney DG, Pieters BCH, Pink RC, Pisetsky DS, Pogge von Strandmann E, Polakovicova I, Poon IKH, Powell BH, Prada I, Pulliam L, Quesenberry P, Radeghieri A, Raffai RL, Raimondo S, Rak J, Ramirez MI, Raposo G, Rayyan MS, Regev-Rudzki N, Ricklefs

FL, Robbins PD, Roberts DD, Rodrigues SC, Rohde E, Rome S, Rouschop KMA, Rughetti A, Russell AE, Saá P, Sahoo S, Salas-Huenuleo E, Sánchez C, Saugstad JA, Saul MJ, Schiffelers RM, Schneider R, Schøyen TH, Scott A, Shahaj E, Sharma S, Shatnyeva O, Shekari F, Shelke GV, Shetty AK, Shiba K, Siljander PRM, Silva AM, Skowronek A, Snyder OL, Soares RP, Sódar BW, Soekmadji C, Sotillo J, Stahl PD, Stoorvogel W, Stott SL, Strasser EF, Swift S, Tahara H, Tewari M, Timms K, Tiwari S, Tixeira R, Tkach M, Toh WS, Tomasini R, Torrecilhas AC, Tosar JP, Toxavidis V, Urbanelli L, Vader P, van Balkom BWM, van der Grein SG, Van Deun J, van Herwijnen MJC, Van Keuren-Jensen K, van Niel G, van Royen ME, van Wijnen AJ, Vasconcelos MH, Vechetti IJ, Veit TD, Vella LJ, Velot É, Verweij FJ, Vestad B, Viñas JL, Visnovitz T, Vukman KV, Wahlgren J, Watson DC, Wauben MHM, Weaver A, Webber JP, Weber V, Wehman AM, Weiss DJ, Welsh JA, Wendt S, Wheelock AM, Wiener Z, Witte L, Wolfram J, Xagorari A, Xander P, Xu J, Yan X, Yáñez-Mó M, Yin H, Yuana Y, Zappulli V, Zarubova J, Žėkas V, Zhang J.-y., Zhao Z, Zheng L, Zheutlin AR, Zickler AM, Zimmermann P, Zivkovic AM, Zocco D, Zuba-Surma EK, Minimal information for studies of extracellular vesicles 2018 (MISEV2018): a position statement of the International Society for Extracellular Vesicles and update of the MISEV2014 guidelines, Journal of Extracellular Vesicles 7(1) (2018) 1535750. [PubMed: 30637094]

[46]. Jiang D, Muschhammer J, Qi Y, Kügler A, De Vries JC, Saffarzadeh M, Sindrilaru A, Beken SV, Wlaschek M, Kluth MA, Suppression of neutrophil-mediated tissue damage—a novel skill of mesenchymal stem cells, Stem Cells 34(9) (2016) 2393–2406. [PubMed: 27299700]

[47]. Munir H, Luu NT, Clarke LS, Nash GB, McGettrick HM, Comparative Ability of Mesenchymal Stromal Cells from Different Tissues to Limit Neutrophil Recruitment to Inflamed Endothelium, PLoS One 11(5) (2016) e0155161. [PubMed: 27171357]

[48]. Liu J, Li P, Zhu J, Lin F, Zhou J, Feng B, Sheng X, Shi X, Pan Q, Yu J, Gao J, Li L, Cao H, Mesenchymal stem cell-mediated immunomodulation of recruited mononuclear phagocytes during acute lung injury: a high-dimensional analysis study, Theranostics 11(5) (2021) 2232–2246. [PubMed: 33500722]

[49]. Li Y.-h., Shen S, Shao T, Jin M.-t., Fan D.-d., Lin A.-f., Xiang L.-x., Shao J.-z., Mesenchymal stem cells attenuate liver fibrosis by targeting Ly6Chi/lo macrophages through activating the cytokine-paracrine and apoptotic pathways, Cell Death Discovery 7(1) (2021) 239. [PubMed: 34518510]

[50]. Li H, Shen S, Fu H, Wang Z, Li X, Sui X, Yuan M, Liu S, Wang G, Guo Q, Immunomodulatory Functions of Mesenchymal Stem Cells in Tissue Engineering, Stem Cells International 2019 (2019) 9671206. [PubMed: 30766609]

[51]. Elisseeff J, Badylak SF, Boeke JD, Immune and Genome Engineering as the Future of Transplantable Tissue, New England Journal of Medicine 385(26) (2021) 2451–2462. [PubMed: 34936741]

[52]. Hussey GS, Dziki JL, Lee YC, Bartolacci JG, Behun M, Turnquist HR, Badylak SF, Matrix bound nanovesicle-associated IL-33 activates a pro-remodeling macrophage phenotype via a non-canonical, ST2-independent pathway, J Immunol Regen Med 3 (2019) 26–35. [PubMed: 31656879]

[53]. Allman AJ, McPherson TB, Badylak SF, Merrill LC, Kallakury B, Sheehan C, Raeder RH, Metzger DW, Xenogeneic extracellular matrix grafts elicit a TH2-restricted immune response, Transplantation 71(11) (2001) 1631–40. [PubMed: 11435976]

[54]. Methe K, Nayakawde NB, Banerjee D, Sihlbom C, Agbajogu C, Travnikova G, Olausson M, Differential Activation of Immune Cells for Genetically Different Decellularized Cardiac Tissues, Tissue Engineering Part A 26(21–22) (2020) 1180–1198. [PubMed: 32484039]

[55]. Van Dyken SJ, Mohapatra A, Nussbaum JC, Molofsky AB, Thornton EE, Ziegler SF, McKenzie AN, Krummel MF, Liang HE, Locksley RM, Chitin activates parallel immune modules that direct distinct inflammatory responses via innate lymphoid type 2 and γδ T cells, Immunity 40(3) (2014) 414–24. [PubMed: 24631157]

[56]. Reese TA, Liang H-E, Tager AM, Luster AD, Van Rooijen N, Voehringer D, Locksley RM, Chitin induces accumulation in tissue of innate immune cells associated with allergy, Nature 447(7140) (2007) 92–96. [PubMed: 17450126]

[57]. Maestas DR, Chung L, Han J, Wang X, Sommerfeld SD, Moore E, Nguyen HH, Mejías JC, Peña AN, Zhang H, Hooks JST, Chin AF, Andorko JI, Berlicke C, Krishnan K, Choi Y, Anderson AE, Mahatme R, Mejia C, Eric M, Woo J, Ganguly S, Zack DJ, Housseau F, Pardoll DM, Elisseeff JH, Helminth egg derivatives as pro-regenerative immunotherapies, bioRxiv (2022) 2022.05.02.490277.

[58]. Griffin DR, Archang MM, Kuan CH, Weaver WM, Weinstein JS, Feng AC, Ruccia A, Sideris E, Ragkousis V, Koh J, Plikus MV, Di Carlo D, Segura T, Scumpia PO, Activating an adaptive immune response from a hydrogel scaffold imparts regenerative wound healing, Nat Mater 20(4) (2021) 560–569. [PubMed: 33168979]

[59]. Heredia Jose E., Mukundan L, Chen Francis M., Mueller Alisa A., Deo Rahul C., Locksley Richard M., Rando Thomas A., Chawla A, Type 2 Innate Signals Stimulate Fibro/Adipogenic Progenitors to Facilitate Muscle Regeneration, Cell 153(2) (2013) 376–388. [PubMed: 23582327]

[60]. Goh YPS, Henderson NC, Heredia JE, Red Eagle A, Odegaard JI, Lehwald N, Nguyen KD, Sheppard D, Mukundan L, Locksley RM, Chawla A, Eosinophils secrete IL-4 to facilitate liver regeneration, Proceedings of the National Academy of Sciences 110(24) (2013) 9914–9919.

[61]. Hart KM, Fabre T, Sciurba JC, Gieseck RL, Borthwick LA, Vannella KM, Acciani TH, de Queiroz Prado R, Thompson RW, White S, Type 2 immunity is protective in metabolic disease but exacerbates NAFLD collaboratively with TGF-β, Science translational medicine 9(396) (2017).

[62]. Kastenschmidt JM, Coulis G, Farahat PK, Pham P, Rios R, Cristal TT, Mannaa AH, Ayer RE, Yahia R, Deshpande AA, Hughes BS, Savage AK, Giesige CR, Harper SQ, Locksley RM, Mozaffar T, Villalta SA, A stromal progenitor and ILC2 niche promotes muscle eosinophilia and fibrosis-associated gene expression, Cell Rep 35(2) (2021) 108997. [PubMed: 33852849]

[63]. Hams E, Armstrong ME, Barlow JL, Saunders SP, Schwartz C, Cooke G, Fahy RJ, Crotty TB, Hirani N, Flynn RJ, Voehringer D, McKenzie ANJ, Donnelly SC, Fallon PG, IL-25 and type 2 innate lymphoid cells induce pulmonary fibrosis, Proceedings of the National Academy of Sciences 111(1) (2014) 367–372.

[64]. Mishra PK, Palma M, Buechel B, Moore J, Davra V, Chu N, Millman A, Hallab NJ, Kanneganti T-D, Birge RB, Behrens EM, Rivera A, Beebe KS, Benevenia J, Gause WC, Sterile particle-induced inflammation is mediated by macrophages releasing IL-33 through a Bruton's tyrosine kinase-dependent pathway, Nature Materials 18(3) (2019) 289–297. [PubMed: 30664693]

[65]. Digiacomo L, Cardarelli F, Pozzi D, Palchetti S, Digman MA, Gratton E, Capriotti AL, Mahmoudi M, Caracciolo G, An apolipoprotein-enriched biomolecular corona switches the cellular uptake mechanism and trafficking pathway of lipid nanoparticles, Nanoscale 9(44) (2017) 17254–17262. [PubMed: 29115333]

[66]. Ogawara K.-i., Furumoto K, Nagayama S, Minato K, Higaki K, Kai T, Kimura T, Pre-coating with serum albumin reduces receptor-mediated hepatic disposition of polystyrene nanosphere: implications for rational design of nanoparticles, Journal of Controlled Release 100(3) (2004) 451–455. [PubMed: 15567509]

[67]. Helder MRK, Stoyles NJ, Tefft BJ, Hennessy RS, Hennessy RRC, Dyer R, Witt T, Simari RD, Lerman A, Xenoantigenicity of porcine decellularized valves, Journal of Cardiothoracic Surgery 12(1) (2017) 56. [PubMed: 28716099]

[68]. Chen G, Qian H, Starzl T, Sun H, Garcia B, Wang X, Wise Y, Liu Y, Xiang Y, Copeman L, Liu W, Jevnikar A, Wall W, Cooper DKC, Murase N, Dai Y, Wang W, Xiong Y, White DJ, Zhong R, Acute rejection is associated with antibodies to non-Gal antigens in baboons using Gal-knockout pig kidneys, Nature Medicine 11(12) (2005) 1295–1298.

[69]. Galili U, Induced anti-non gal antibodies in human xenograft recipients, Transplantation 93(1) (2012) 11–6. [PubMed: 22146315]

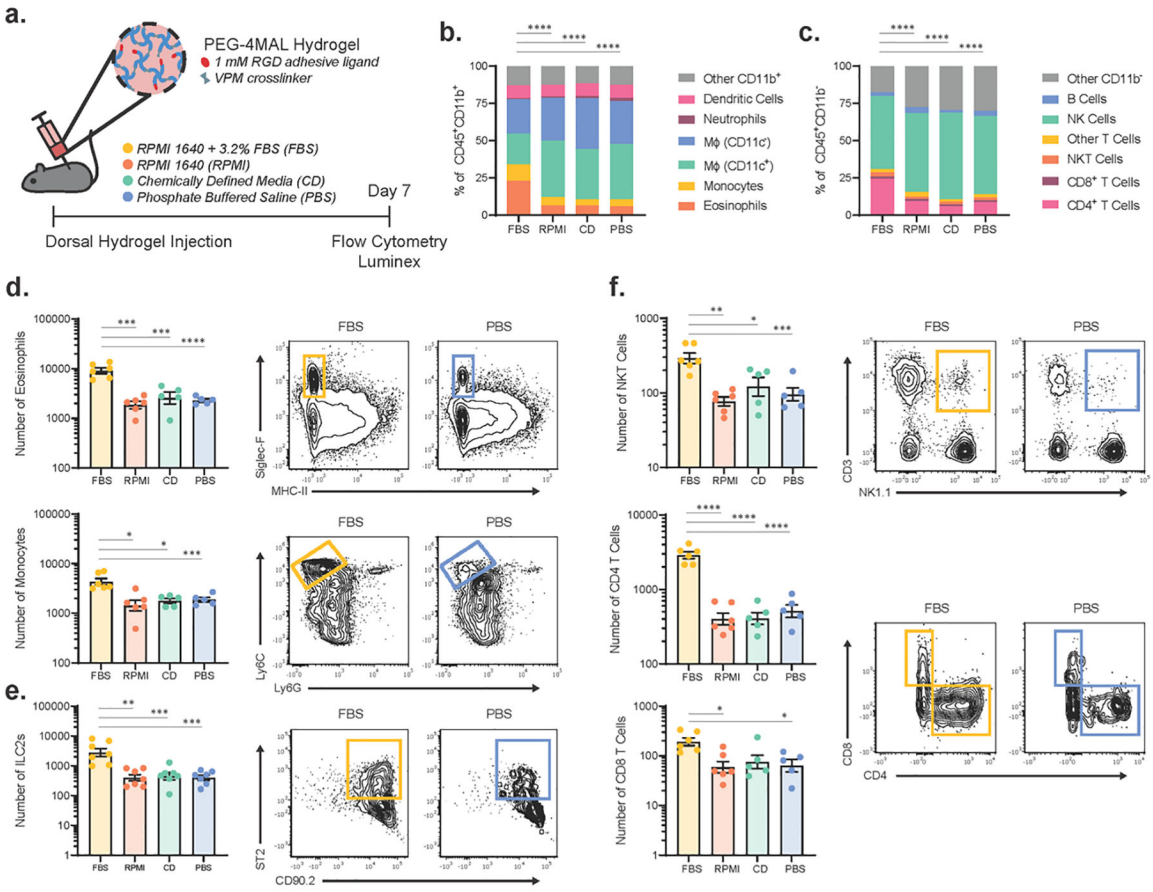

Figure 1. FBS-containing hydrogels induce an immune response with increased eosinophil, ILC2, and CD4$^+$ helper T cell recruitment.

(**a**) Schematic of experimental design. PEG-4MAL hydrogels containing RPMI 1640 + 3.2% MSC-qualified FBS (FBS), RPMI 1640 (RPMI), Xcell Chemically Defined Media (CD), or PBS were injected subcutaneously into the mouse dorsum. On day 7, hydrogels were explanted and the immune response was analyzed via flow cytometry and Luminex multiplex ELISA. Proportion of different cell populations in the (**b**) myeloid (CD11b$^+$) and (**c**) lymphoid (CD11b$^-$) compartments within the dorsal hydrogels as analyzed by flow cytometry. Indicated cell population percentages are based on the average number of cells in n=6 samples per group. Statistical differences were detected using individual chi-square contingency tests (FBS vs. all other groups) with Bonferroni correction. ****p<0.0001. Number of immune cells in (**d**) CD11b$^+$ myeloid, (**e**) Lin$^-$ (CD3, CD4, CD11b, CD11c, NK1.1, CD19, Ly6G) ICOS$^+$CD90.2$^+$ST2$^+$ ILC2, and (**f**) CD11b$^-$ lymphoid populations with significant differences between hydrogels containing FBS and those without (n=5–7); mean ± SEM. A one-way ANOVA was used to detect statistical differences followed by Tukey's multiple comparisons test with adjustment for multiple comparisons. Data in (**d-f**) were log transformed prior to statistical analysis. *p<0.05, **p<0.01, ***p<0.001, ****p<0.0001.

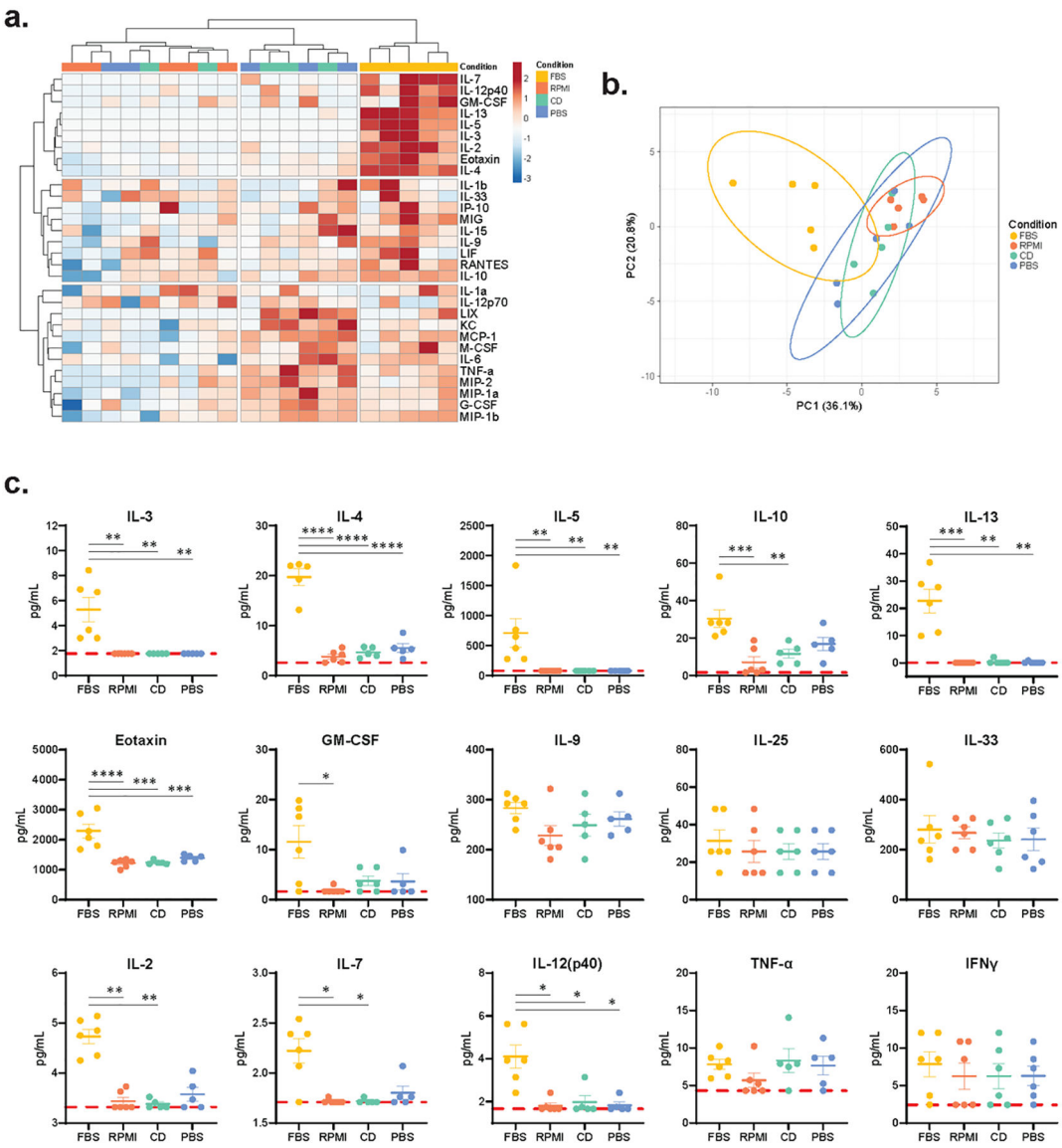

Figure 2. The immune response induced by FBS-containing hydrogels is characterized by increased local concentrations of cytokines associated with type 2 immunity.

Day 7 hydrogel explants were digested and a Luminex bead-based multiplex ELISA was run to analyze the local cytokine milieu. (**a**) Heatmap with two-way hierarchical clustering using Ward's method with Euclidian distances shows distinct clustering of FBS-containing dorsal hydrogels based on local cytokine secretion. Scale bar represents data that has been log transformed, unit variance scaled, and mean centered. (**b**) Principal component analysis of cytokines within dorsal hydrogels. Principal component 1 and principal component 2 are displayed on the X- and Y-axes and explain 36.1% and 20.8% of the variance, respectively. 95% prediction ellipses are also plotted. (**c**) Cytokines with significantly different local concentrations, as well as key type 1 and type 2 immune response cytokines with no significant differences in concentrations (n=6 samples per group). Red, dashed line indicates the limit of detection of the Luminex MAGPIX System. A one-way ANOVA was used to detect statistical differences followed by Tukey's multiple comparisons test

for IL-4, Eotaxin, IL-9, IL-25, and IL-33. For all other cytokines, a Kruskal-Wallis test was used followed by Dunn's multiple comparison test. *p<0.05, **p<0.01, ***p<0.001, ****p<0.0001.

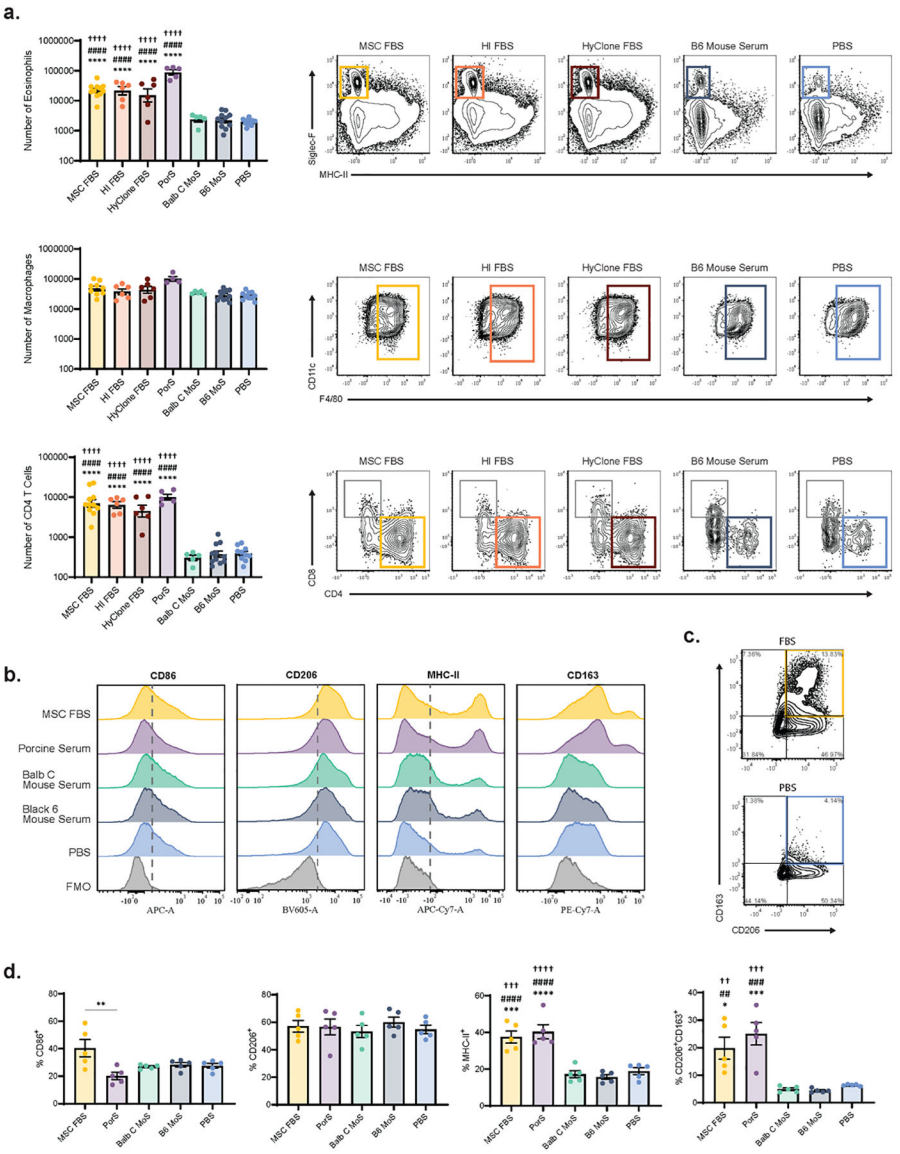

Figure 3. This type 2 immune response is specific to xenogeneic serum proteins.

PEG-4MAL hydrogels containing RPMI 1640 + 3.2% MSC-qualified FBS (MSC FBS), RPMI 1640 + 3.2% heat inactivated FBS (HI FBS), RPMI 1640 + 3.2% HyClone FBS (HyClone FBS), RPMI 1640 + 3.2% Porcine Serum (PorS), RPMI 1640 + 3.2% BALB/c mouse serum (BALB/c MoS), RPMI 1640 + 3.2% C57BL/6J mouse serum (B6 MoS), or PBS were injected subcutaneously into the mouse dorsum. On day 7, hydrogels were explanted and the infiltrating immune cells were analyzed via flow cytometry. (**a**) Number of infiltrating Siglec-F$^+$ eosinophils, F4/80$^+$ macrophages, and CD3$^+$CD4$^+$ T cells as determined by flow cytometry (n=5–11); mean ± SEM. (**b**) Expression of CD86, CD206, MHC-II, and CD163 on F4/80$^+$ macrophages. Grey, dashed line represents the positive gate, determined by FMOs. Representative of 3 independent experiments. (**c**) Flow gates (gated on F4/80$^+$ cells) used to determine the population of CD206$^+$CD163$^+$ double positive macrophages. Quadrants were drawn based on FMOs. (**d**) Frequency of F4/80$^+$

macrophages positive for CD86, CD206, MHC-II, or $CD206^{+}CD163^{+}$ double positive (n=5); mean ± SEM. A one-way ANOVA was used to detect statistical differences followed by Tukey's multiple comparisons test with adjustment for multiple comparisons. Data in (**a**) was log transformed prior to ANOVA analysis. *p<0.05, ***p<0.001, ****p<0.0001 vs. PBS; $^{\#\#}$p<0.01, $^{\#\#\#}$p<0.001, $^{\#\#\#\#}$p<0.0001 vs. B6 MoS; ††p<0.01, †††p<0.001, ††††p<0.0001 vs. BALB/c MoS.

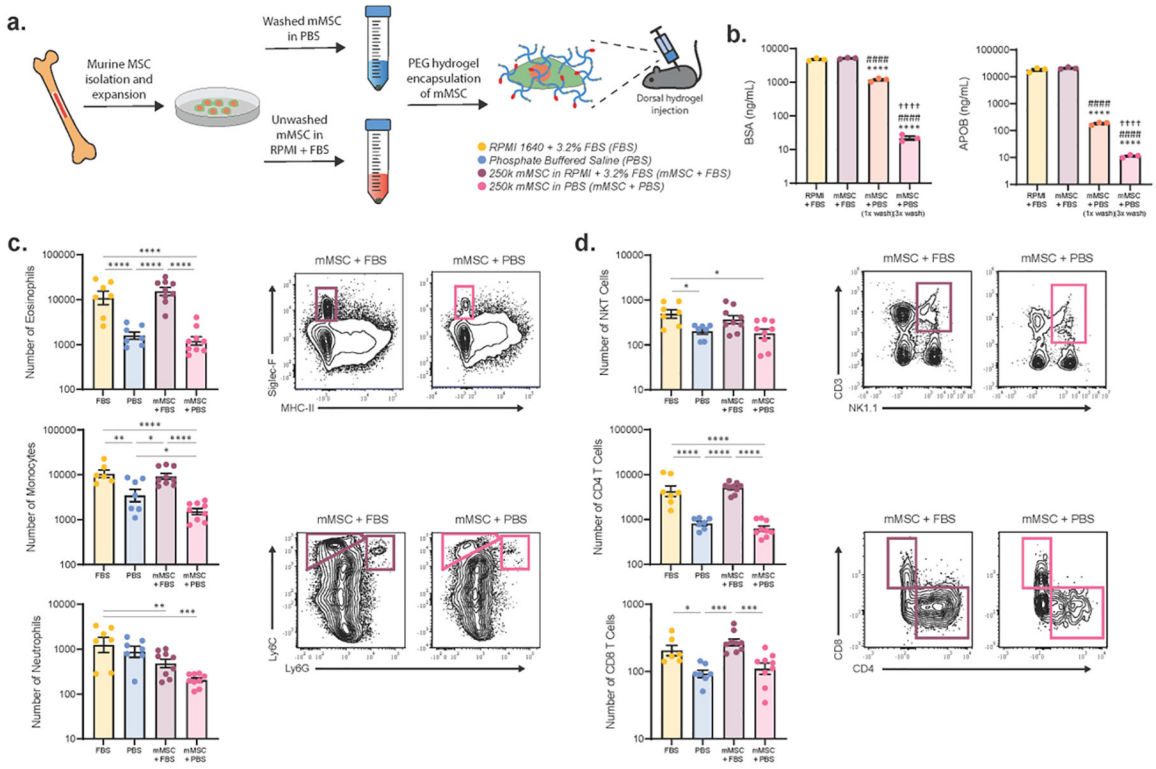

Figure 4. Washing mMSCs before implantation significantly reduces the local serum immune response.

(**a**) Schematic of experimental design for studies involving mMSCs. mMSCs were isolated from C57BL/6J mouse bone marrow and expanded *ex vivo* in media containing MSC-qualified FBS. mMSCs washed 3 times in PBS or unwashed mMSCs were incorporated into a PEG-4MAL hydrogel solution and injected subcutaneously into the mouse dorsum. Cell-free hydrogels containing either MSC-qualified FBS or PBS were included as controls. On day 7, hydrogels were explanted and the immune response was analyzed via flow cytometry. (**b**) Concentration, as measured by plate ELISA, of serum components BSA and bovine APOB in cell suspensions of *ex vivo* expanded mMSCs following washing the cell pellet either once or 3 times with 15 mL of PBS. Unwashed cell pellet in complete media (RPMI + 3.2% MSC-qualified FBS) and complete media without cells were included as controls. Data was log-transformed and a one-way ANOVA was used to detect statistical differences followed by Tukey's multiple comparisons test with adjustment for multiple comparisons. ****$p<0.0001$ vs. RPMI + FBS; $^{\#\#\#\#}p<0.0001$ vs. mMSC + FBS; $^{\dagger\dagger\dagger\dagger}p<0.0001$ vs. mMSC + PBS (1x wash). Number of infiltrating (**c**) myeloid and (**d**) lymphoid cells in populations with significant differences between samples containing FBS and those without (n=6–9); mean ± SEM. A one-way ANOVA was used to detect statistical differences followed by Tukey's multiple comparisons test with adjustment for multiple comparisons. Data in (**c, d**) were log transformed prior to ANOVA analysis. *$p<0.05$, **$p<0.01$, ***$p<0.001$, ****$p<0.0001$.

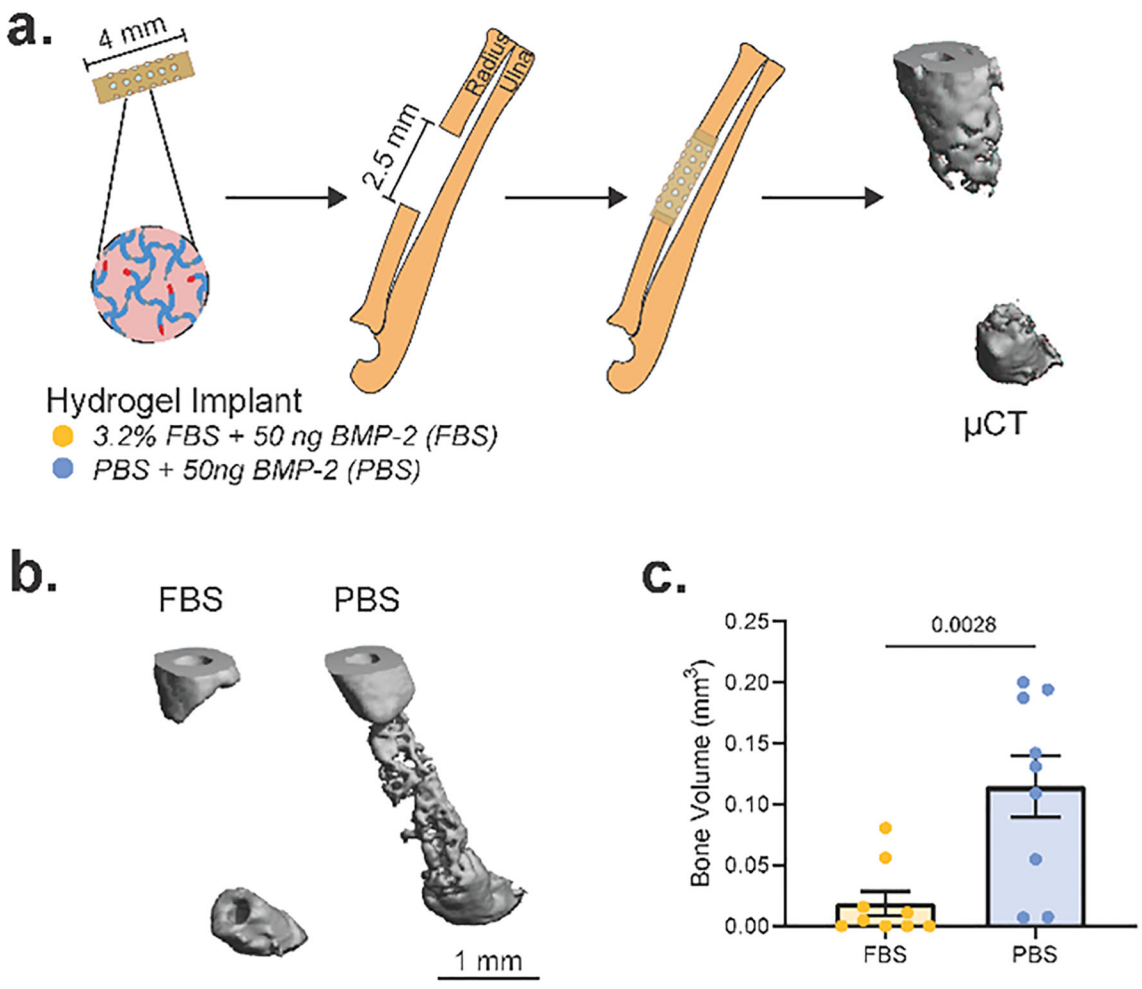

Figure 5. FBS impairs biomaterial-directed bone repair outcomes.

(**a**) Schematic of murine radial segmental defect model. PEG-4MAL hydrogels containing 50 ng BMP-2 and either RPMI 1640 + 3.2% MSC-qualified FBS (FBS) or PBS as the buffer component were cast inside 4 mm polyimide tubes. 2.5 mm unilateral critical-sized radial defects were created in C57BL/6J mice and the hydrogel-containing implant tube was introduced into the defect site. 4 weeks post-surgery, bone volume was analyzed by micro-computed tomography. (**b**) Representative 3D μCT reconstructions of week 4 defects. (**c**) μCT calculated bone volume within the middle 2 mm of the radial defect (n=9 over 2 independent experiments); mean ± SEM. Differences in bone volume were calculated by a two-tailed t-test.

Table 1.

Sera used in study.

Serum	Manufacturer
MSC-qualified FBS, not heat inactivated	Gibco, 12662029
FBS, heat inactivated	Corning, 35–011-CV
HyClone FBS characterized, heat inactivated	Cytiva, SH30071.01
Porcine Serum	Innovative Research, IGPCSER100ML
C57BL/6J Mouse Serum	Innovative Research, IGMSC57SER10ML
BALB/c Mouse Serum	Innovative Research, IGMSBCSER10ML

Table 2.

Antibodies used in flow cytometry panels.

Myeloid Flow Panel			
Target (anti-mouse x)	**Fluorochrome (Cytometer Filter)**	**Company, Catalog Number**	**Dilution**
CD45	PE Dazzle (PI)	BioLegend, 103146	1:100
CD11b	PerCP-Cy5.5	BioLegend, 101228	1:100
CD170 (Siglec-F)	PE	BioLegend, 155506	1:100
I-A/I-E (MHC-II)	APC Fire 750 (APC-Cy7)	BioLegend, 107652	1:100
Ly6C	BV711	BioLegend, 128037	1:100
Ly6G	BV510	BioLegend, 127633	1:100
CD11c	BV786	BioLegend, 117336	1:100
F4/80	FITC	BioLegend, 123108	1:100
CD163	PE-Cy7	BioLegend, 155319	1:100
CD86	APC	BioLegend, 105012	1:100
CD206	BV605	BioLegend, 141721	1:100
Lymphoid Flow Panel			
Target (anti-mouse x)	**Fluorochrome (Cytometer Filter)**	**Company, Catalog Number**	**Dilution**
CD45	FITC	BioLegend, 103108	1:200
CD3	PE Dazzle (PI)	BioLegend, 100246	1:200
CD4	APC	BioLegend, 100412	1:100
CD8a	PerCP-Cy5.5	BioLegend, 100734	1:200
CD11b	V500	BD Biosciences, 562127	3:200
NK1.1	BV650	BioLegend, 108736	1:200
CD19	BV786	BioLegend, 115543	3:200
ILC2 Flow Panel			
Target (anti-mouse x)	**Fluorochrome (Cytometer Filter)**	**Company, Catalog Number**	**Dilution**
CD45	PE Dazzle (PI)	BioLegend, 103146	1:100
CD3	FITC	BioLegend, 100203	1:100
CD4	FITC	BioLegend, 100405	1:100
CD11b	FITC	BioLegend, 101205	1:100
CD11c	FITC	BioLegend, 117305	1:100
NK1.1	FITC	BioLegend, 108705	1:100
CD19	FITC	BioLegend, 152403	1:100
Ly6G	FITC	BioLegend, 127605	1:100
CD278 (ICOS)	APC	BioLegend, 107712	1:100
CD90.2	PerCP-Cy5.5	BioLegend, 105338	1:100
IL-33Rα (ST2)	PE-Cy7	BioLegend, 146610	1:100